Tong *et al.*
European Journal of Medical Research (2025) 30:145
https://doi.org/10.1186/s40001-025-02388-8

European Journal
of Medical Research

RESEARCH

Open Access

Umbilical cord blood-derived platelet-rich plasma as a coating substrate supporting cell adhesion and biological activities of wound healing

Thanh-Hai Tong[1], Xuan-Hai Do[2], Thanh-Thao Nguyen[3], Bich-Hanh Pham[3], Quang-Dung Le[3], Xuan-Hung Nguyen[4,5,6], Nhung Thi My Hoang[3], Thu-Huyen Nguyen[5], Nam Hoang Nguyen[3] and Uyen Thi Trang Than[4,5*]

Abstract

Background Platelet-rich plasma (PrP) is a blood derivative with positive roles in regenerative medicine, particularly in wound healing. Evidence has been reported for using peripheral blood-derived PrP in disease treatments, but umbilical cord blood (UCB)-derived PrP remains limited. Thus, we investigate the roles of UCB-derived PrP in cellular behaviours in vitro and in wound healing in vivo models.

Methods We used 2D and 3D cell culture models to investigate the role of UCB-derived PrP gels in stimulating the attachment, proliferation, migration, and spheroid formation of umbilical cord-derived mesenchymal stem cell (UCMSC) and human dermal fibroblast (hFB). In addition, immunoassay and PCR were used to understand the enrichment of growth factors in UCB-derived PrP and the change of ECM genes in PrP-treated cells. Finally, a rat model was used to investigate the cutaneous wound healing process.

Results UCB-derived PrP gels were enriched with platelet-derived growth factor-BB (PDGF-BB) (3394.1 ± 2658.3 pg/mL), vascular endothelial growth factor-A (VEGF-A) (282.0 ± 53.0 pg/mL), hepatocyte growth factor (HFG) (762.7 ± 117.5 pg/mL), and fibroblast growth factor 2 (FGF-2) (17.734 ± 8 pg/mL). In addition, these UCB-derived PrP gels promoted cell attachment (> 154 % and > 117 % for UCMSCs and hFBs, respectively), proliferation (UCMSCs > 121 % and hFBs > 117 % at all time points), migration increased by 27 % and 26 % for UCMSCs and hFBs, and spheroid formation and fusion compared to the control. UCB-derived PrP gels also induced different expression of ECM genes, including COL1, COL3, HAS1, HAS2, HAS3, and ENL, in both UCMSCs and hFBs. Finally, this product from UCBs could enhance the wound healing process in excised skin rat models by reducing the wound area by 80 % compared to 27 % in controls after 14 days.

Conclusions UCB-derived PrP gels facilitate cell behaviours in vitro, including cell adhesion, growth, and migration. In addition, in animal models, UCB-derived PrP reduced the wound healing time and enhanced the completion of skin tissues by increasing granulation tissue formation and reducing neutrophils at wound sites. These UCB-derived

*Correspondence:
Uyen Thi Trang Than
v.uyenttt@vinmec.com
Full list of author information is available at the end of the article

PrP gels will be used to support spheroid formation that will be used as biomaterials for 3D printing, engraftment, and wound healing treatment.

Keywords UCB-derived PrP, Cell attachment, Surface coating, Wound healing, Spheroids, Proliferation, Migration

Introduction

Platelet-rich plasma (PrP) is an autologous blood product acquired from part of the plasma fraction obtained through the centrifugation of whole blood, which has a higher platelet concentration than circulating blood [1]. Previous studies indicate that PrP exhibits antimicrobial actions against various pathogens, including *Candida albicans*, *Cryptococcus neoformans*, *Escherichia coli*, and *Staphylococcus aureus* [2–4]. Besides that function, PrP has been reported to be involved in regenerative medicine due to their rich reservoir of bioactive components, including growth factors, proteins and peptides, chemokines, cytokines, and fibrin scaffolding, which are all directly sourced from the patient's blood [2]. The prominent growth factors that are associated with regeneration pooling in PrP can be mentioned are PDGF, epidermal growth factor (EGF), FGF, transforming growth factor beta 1 (TGF-β1), insulin growth factor-1 (IGF-1), keratinocyte growth factor (KGF), VEGF, etc. [5]. Importantly, those factors, after being released, stimulate cell migration, proliferation, and differentiation for the initiation of the healing of damaged tissues [5]. In addition, PrP gels contain fibronectin, vitronectin, fibrinogen, and sphingosine-1-phosphate, which are essential for the remodeling phase of the wound healing process [6].

Using PrP technology in wound healing presents many advantages, positioning it as an appealing option in regenerative medicine. Notably, the methodology associated with PrP is characterized by its simplicity, safety, and cost-effectiveness [7]. Although peripheral autologous PrP has been demonstrated to be safe and effective in wound healing and other disease conditions, the use of UCB-derived PrP as a therapeutic agent has some benefits in efficacy and large-scale production and standardization. A widely available resource of UCB for PrP production can be easily obtained from donors; in addition, maintaining a consistent, high-quality, and standardization of products necessitates robust donor screening and the establishment of efficient cord blood banking systems. Besides that, UCB-PrP also owns its benefits of homologous sources that are not linked to the physiological states of patients [8]. The use of autologous PrP in elders, newborns, children, or immune-diseased patients who require blood collection repeats is not appropriate in clinical practices. Moreover, it is proposed that the preparation process could be further optimized to control the dose of bioactive molecules provided by PrP, which is essential for its therapeutic efficacy [5]. In this regard, UCB-PrP contains higher levels of growth factors and anti-inflammatory cytokines [8, 9], while autologous PrP contains pro-inflammatory cytokines [10]. Despite a few studies that have compared peripheral blood PrP and UCB-derived PrP, including their components and efficacy for disease treatments [8, 9, 11], more applications of this potential UCB-derived PrP are unclear. Finally, the demand for commercially available off-the-shelf products enables the potential of UCB-PrP in practice.

Thus, this study aims to explore the potential of using UCB-derived PrP gels in cell interaction in vitro and wound healing. We hypothesize that UCB-derived PrP will facilitate cell attachment, proliferation, and migration through different models employing human UCMSCs and FBs in 2D and 3D cultures. In addition, we hypothesize that UCB-derived PrP gels will stimulate wound closure and complete the healed tissues in vivo excision wound model in rats.

Materials and methods

UCB-derived PrP preparation

UCB was drawn directly from the umbilical cord of the infant right after the baby was born and preserved at 4 °C upon delivery. Collected cord blood was processed within 8 h of the collection after disinfecting blood bags with 70 % ethanol. Whole blood was transferred into 15 mL centrifuge tubes and centrifuged at 3000 RPM for 20 min (80-2B Centrifuge, Jangsu Xinkang Medical, China), resulting in three separate layers, including bottom layer of hematocrit layer, intermediate buffy coat layer, and top plasma layer. The middle layer, considered inactivated PrP, was collected (2 mL from 10 mL UCB) and transferred into a new tube before being supplemented with $CaCl_2$ and thrombin to activate platelets. The mixture was then incubated at 4 °C for 30 min. During this time, platelets in inactivated PrP were activated by $CaCl_2$ (10 %) and thrombin (8 %), and then PrP was gradually transformed from liquid to gel. This umbilical cord blood-derived PrP (UCB-PrP) gel was stored at 4 °C for up to 2 h or - 80 °C for a longer time for further evaluation. The density of platelets in the whole blood and inactivated UCB-PrP was determined on the hematology analyzer Model Z3 (Zybio, China).

Growth factor analysis using Luminex assay

The amount of four growth factors, including FGF-2, HGF, PDGF-BB, and VEGF-A, in UCB-PrP were measured by Luminex assay using ProcartaPlex™ Multiplex Immunoassays (Human Custom ProcartaPlex 4-Plex Kit, ThermoFisher, Massachusetts, US). Briefly, 50 µL Magnetic Beads were added into each well and washed using a Wash Buffer. Then, 50 µL Antigen Standard, blank, and PrP samples were added and incubated for 2 h before being washed by washing buffer to remove unbound reagents. Details of reagent preparation and procedures followed the manufacturer's instructions. The luminescent signal, representing the growth factor's concentrations, was detected using the Luminex™ 100/200™ system with xPONENT 3.1 software.

Cell culture and surface coating

Human fibroblasts (hFBs) and umbilical cord-derived mesenchymal stem cells (UCMSCs) were cultured in conventional media (DMEM/F12 supplemented with 10 % FBS) [12–14]. Non-coated plates used for cell cultures were coated with surface coating solutions, including either commercial product of CELLstart™ CTS™ (CELLstart) or UCB-PrP gel and non-coated plates were used as the control. CELLstart™ CTS™ was diluted at 1:100 with PBS (*v*:*v*). UCB-PrP gel was diluted with PBS at different ratios (*v*:*v*) of 2:100 (2 %), 1:100 (1 %), and 0.3:100 (0.3 %). Surface coating solutions were applied onto 96-well culture plates to cover the culture well surface completely. The plates were incubated at 37 °C in a humidified atmosphere of 5 % CO_2 for 1 h. Any excess coating solutions were discarded before adding the cells.

Cell attachment and proliferation assays

An MTT (3-(4,5-Dimethylthiazol-2-yl)-2,5-Diphenyltetrazolium Bromide) assay (Promega, Madison, WI, USA) was performed to quantify the concentration of cells attaching to the surface of culture flasks and cell proliferation at different coating conditions. The metabolic active cells convert MTT into a purple product of insoluble formazan that is then solubilized by dimethyl sulfoxide (DMSO) and can be quantified and correlated with living cell number [15]. UCMSCs were plated on pre-coated 96-well plates at 2800 cells per well and incubated at 37 °C and 5 % CO_2. Cell viability was examined for cellular adhesion at a 4 h and cell proliferation at 4, 24, 48, and 72 h. After each assessment timepoint, 15 µL of dye solution of the MTT labeling reagent (final concentration 0.5 mg/mL) was added to each well and incubated at 37 °C for 4 h in a humidified CO_2 incubator. Then, 100 µL of solubilization/stop solution was added to each well, and the absorbance was measured at 570 nm using an ELISA plate reader (BioTech Power Wave XS, Winooski, VT, USA). The experiments were performed for three biological repeats.

Wound healing assay

Cells ($n=3$) were cultured in 24-well plates at a density of 8000 cells/cm^2 (equivalent to 15,200 cells/well). When cells expanded to cover the entire surface of the culture plate (100 % confluency), mitomycin (10 µg/mL) was added into each well for 2 h to inhibit cell proliferation before scratch wounds were created using a scratcher (SLP, Korea). The migration of cells to close the scratch was observed and captured by optical microscopy at time points of 0, 12, 24, 36, and 48 h. Image results were analyzed using ImageJ software (version 1.46r).

Multicellular spheroid cultures

Hanging drop formation

Spheroids were formed using the hanging drop method in 100 mm culture dishes, where 2.5×10^6 cells/mL (cells counted using trypan blue method) were divided into equal volumes in 1.5 mL Eppendorf tubes with different coating substrates to get the concentration of 1 % PrP and 1 % CELLstart™. The bottom of the dish was filled with PBS 1X to protect drops from evaporation. Turned the lid upside down and deposited 20 µL drops containing 50,000 cells onto the lid. Afterward, the lid was inverted onto the bottom of the dish filled with PBS 1X and incubated at 37 °C and 5 % CO_2. Spheroids were formed in approximately 24 - 36 h. Experiments were performed for five biological repeats.

Spheroid fusion

Quick and efficient spheroid fusion is one of the significant factors for rapid tissue biofabrication, especially through bioprinting. The 96-well U-bottomed plate was coated with polyHEMA (2-hydroxyethyl methacrylate) (Corning, USA) dissolved in an ethanol solution to prevent cells from attaching to spheroids. 30 µL polyHEMA solution was added into each well, and then the plate was opened to evaporate under sterile conditions. Two spheroids were placed in proximity to ensure an initial touch to synchronize all distance conditions in each well. This process, termed doublets fusion, was then observed with an inverted microscopy and imaged by a digital camera.

The measurements of the spheroid fusion followed the method described by Moor et al. [16]. The doublet fusion capacity was determined based on the doublet length, width, contact length, perimeter, and intersphere angle. The squared aspect ratio of the contact length of doublet (D) over the diameter of the spheroid (d) was calculated to assess the spheroid fusion process. All measurements

were performed for five biological repeats and conducted using ImageJ software (Java).

Total RNA extraction and quantitative reverse transcription–PCR

Cells were collected from 2 and 3D cultures in different experimental conditions ($n=3$). Then, total RNA was extracted following the phenol-chloroform method using Trizol™ (Thermo Scientific, Massachusetts, USA). The lysis mixture was added with chloroform and incubated at RT for phase separation. The aqueous phase was collected and incubated with isopropanol overnight at - 20 °C. The resulting total RNA was pelleted through centrifugation, subjected to two washes with RNase-free 75 % ethanol, air-dried, and then resuspended in RNase-free water.

Quantified RNAs were used for cDNA preparation using SuperScript™ IV Reverse Transcriptase (Thermo Scientific, Massachusetts, USA) following the manufacturer's protocol. The resulting cDNA products were then subjected to qPCR reaction, using specific-designed primers targeting the respective RNAs of COL1, COL3, HAS1, HAS2, HAS3, and Elastin. GAPDH served as an internal control (primer sequences are listed in Table 1). The reaction was run for 40 thermal cycles (denaturation: 94 °C/15 s, annealing: 55 °C/30 s, and extension: 70 °C/34 s) and melt curve stage (95 °C/15 s, 60 °C/60 s, 95 °C/30 s, 60 °C/15 s). The $2^{-\Delta\Delta Ct}$ method was applied to calculate the relative fold gene expression of samples.

Animal model for skin wound healing

Wistar male rats (Rattus norvegicus) used for wound healing examinations were provided by the Experimental Animal Center, Military Medical Academy. Rats were fed a standard diet with food and normal drinking water and housed in the laboratory at a consistent condition of 25 °C, 55 % relative humidity, and a 12 h/12 h light/dark cycle. Animals were anesthetized with an intraperitoneal injection of 60 mg/kg body-weight ketamine HCl (Rotexmedica GmbH Arzneimittelwerk, Germany). The back skin was shaved and sterilized, then drawn circles symmetrically across the spine. A blade 11 was used to make a small 0.5 cm long incision on the skin, and then Mayo scissors curved 14 cm long to cut the skin following the drawn line and remove all layers of skin. Finally, two circular and full-thickness 1.5 - 2.0 cm diameter cutaneous wounds were symmetrically created across the spine, with one site treated with 200 µL UCB-PrP gel and the other with betadine as control. The wounded sites were kept 1 cm away from the spine. Each rat was kept individually per cage after making the wound model. Twenty-four rats were randomly divided into three groups ($n=7$ per group) corresponding to three time points of assessment on days 3, 7, and 14 post-model creation. Photographs were taken at each assessment time point.

The image analysis software (ImageJ) was used to measure the closed wound area [17]. The following equation determined the wound healing rate (% of closed wound area): W % (Percent of closed wound area) $=(W0-W\mathrm{t})/\mathrm{W}0\times100$ %, where: $W0$ is the initial wound area and Wt is the residual wound area.

On days 3, 7, and 14, whole back skin samples were collected and fixed in 10 % formalin for 24 h and processed for histological analysis. Briefly, specimens underwent dehydration with 95 % and 70 % alcohol. After embedding the paraffin blocks, samples were cut into 3 - 4 µm-thick sections and placed on glass slides for H&E staining. Samples were stained with Hematoxylin for 10 min, then Eosin for 30 s, followed by a lamen cover and observed under a Zeiss AxioPlan 2 Imaging Microscope (Carl Zeiss, Germany). The analysis included evaluating the presence of ulcers, granulation tissue, infiltrating leukocytes, and congested blood capillaries.

Table 1 Primer sequences

Gene name	Primer	Sequence	Size (bp)
COL1	Forward	CCTGTCTGCTTCCTGTAAACTC	101
	Reverse	GTTCAGTTTGGGTTGCTTGTC	
COL3	Forward	GAAGGGCAGGGAACAACTTG	243
	Reverse	TTTGGCATGGTTCTGGCTTC	
ELN	Forward	GGCCATTCCTGGTGGAGTTCC	106
	Reverse	AACTGGCTTAAGAGGTTTGCCTCCA	
HAS1	Forward	ACGTGCGGATCCTTAACCCT	136
	Reverse	AGGCCTAGAGGACCGCTGAT	
HAS2	Forward	GTCATGGGCAGAGACAAATCAG	108
	Reverse	CGTTACGTGTTGCGAGCTTTC	
HAS3	Forward	GGGCATTATCAAGGCCACCTA	137
	Reverse	CAGATTTGTTGATGGTAGCAATGG	
GAPDH	Forward	GGTGTGAACCATGAGAAGTATGA	123
	Reverse	GAGTCCTTCCACGATACC AAAG	

Statistical analysis

Statistical analysis was performed using Microsoft Excel 2019 (Microsoft, United States) and GraphPad Prism (v.8.4.3; GraphPad Software, San Diego, California). Data were collected from at least three biological replicates. The measurement data are presented as the Mean ± SD and analyzed by one-way variance analysis (ANOVA), followed by a Tukey multiple comparison test. $p<0.05$ was considered a statistically significant difference.

Results

UCB-PrP gel characterization

UC-PrP gels generated from the inactivated PrP had a platelet (PLT) concentration of $6.5 \pm 1.5 \times 10^9$/mL, eight times higher than that in the whole blood with a concentration of $0.8 \pm 0.05 \times 10^9$/mL (Fig. 1A). The PLT recovery efficiency was 95 ± 1.2 %, indicating that our protocol is efficient in harvesting and activating UCB-PrP gels.

In addition, we measured growth factors, including FGF-2, HGF, PDGF-BB, and VEGF-A, presented in UCB-PrP gels. Results showed that all four factors of FGF-2, HGF, PDGF-BB, and VEGF-A have been detected with high levels in UCB-PrP gels. Among them, FGF-2 was detected with the lowest level (17.734 ± 8 pg/mL), followed by VEGF-A (282.0 ± 53.0 pg/mL) and HGF (762.7 ± 117.5 pg/mL), while PDGF-BB was detected with the highest level (3394.1 ± 2658.3 pg/mL) (Fig. 1B). These data indicated that UCB-PrP gels have potential as regenerative medicine.

UCB-PrP gels induced cell adhesion and proliferation

UCMSCs and hFBs are adherent cells that rely on surface attachment for growth. Therefore, we evaluated the impact of utilizing UCB-PrP gels as a coating material to promote the adhesion of these cells to the culture flask surface. At 4 h post-seeding, most of the cells adhered to the culture flasks, albeit with some cells remaining floated in the culture medium (Fig. 2A). Quantitative analysis revealed that UCB-PrP gels at concentrations of 1 % and 2 % functioned as effective coating substrates, resulting in a higher number of adherent cells (UCMSCs: 154.9 ± 17.3 % and 155.7 ± 19.3 %; hFBs: 121.3 ± 6.7 % and 117.8 ± 8.2 %, respectively, PrP 1 % and 2 %) compared to the non-coating control (100 %). However, a lower concentration of UCB-PrP (0.3 %) did not enhance the cell attachment after 4 h of seeding (Fig. 2B).

Furthermore, the UCB-PrP gel-coating substrate showed an ability to promote cell growth. Both UCMSCs and hFBs expressed a superior proliferation compared to the controls (100 %) across three assessment time points at 24 h (UCMSCs: 124.5 ± 8.5 % (PrP 0.3 %), 126.5 ± 9.8 % (PrP 1 %), 135 ± 14.5 % (PrP 2 %); hFBs: 126.5 ± 15.3 % (PrP 0.3 %), 125 ± 9.2 % (PrP 1 %), 120 ± 7.5 % (PrP 2 %)), 48 h (UCMSCs: 129 ± 10.2 % (PrP 0.3 %), 129 ± 11.9 % (PrP 1 %), 138.5 ± 9.3 % (PrP 2 %); hFBs: 133.6 ± 9.1 1% (PrP 0.3 %), 132.5 ± 13.6 % (PrP 1 %), 117.5 ± 10.4 % (PrP 2 %)), and 72 h (UCMSCs: 121.5 ± 9.5 % (PrP 0.3 %), 127.5 ± 9.7 % (PrP 1 %), 132.7 ± 16.5 % (PrP 2 %); hFBs: 127.9 ± 14.8 % (PrP 0.3 %), 128.7 ± 9.5 % (PrP 1 %), 125 ± 12.3 % (PrP 2 %)) (Fig. 2C). However, the tendency

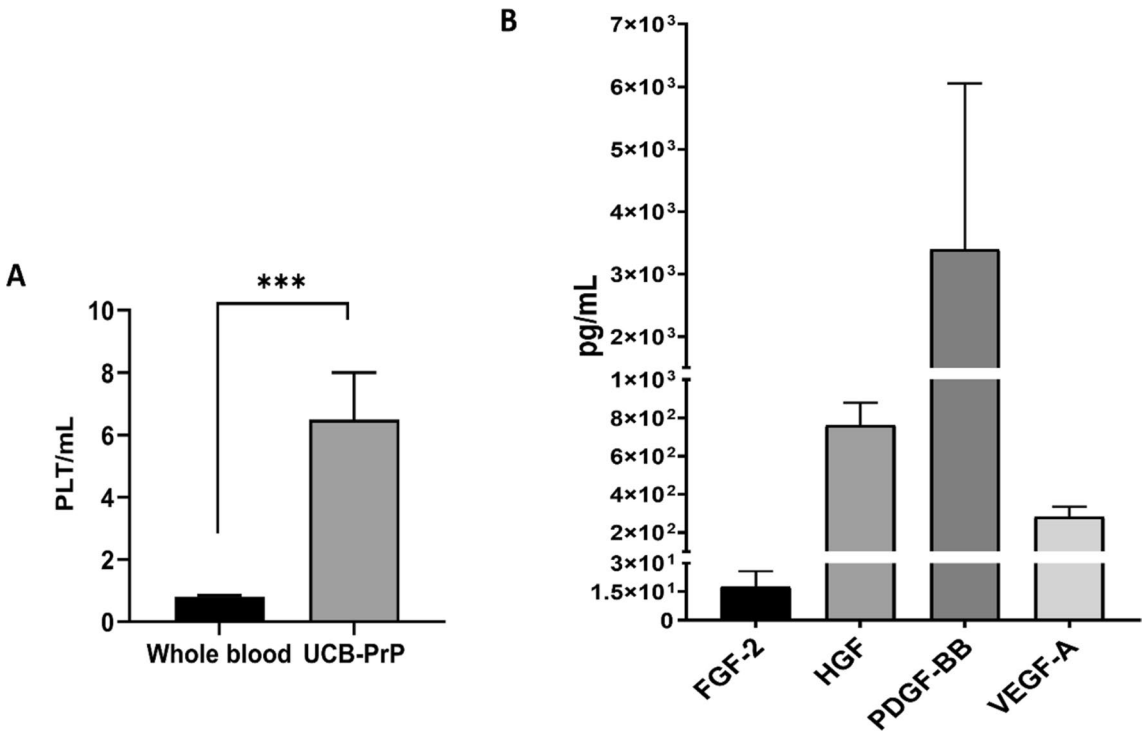

Fig. 1 UCB-PrP gel characterization. **A** Recovery efficacy of platelet (PLT) from whole blood, where the concentration of PLT was eight times higher in the inactivated UCB-PrP compared to whole blood sample ($n = 5$). **B** Quantifying growth factors within UCB-PrP gels, including FGF-2, HGF, PDGF-BB, and VEGF-A using Luminex assay ($n = 3$). Notably, PDGF-BB exhibited the highest concentration. ***indicates $p < 0.001$

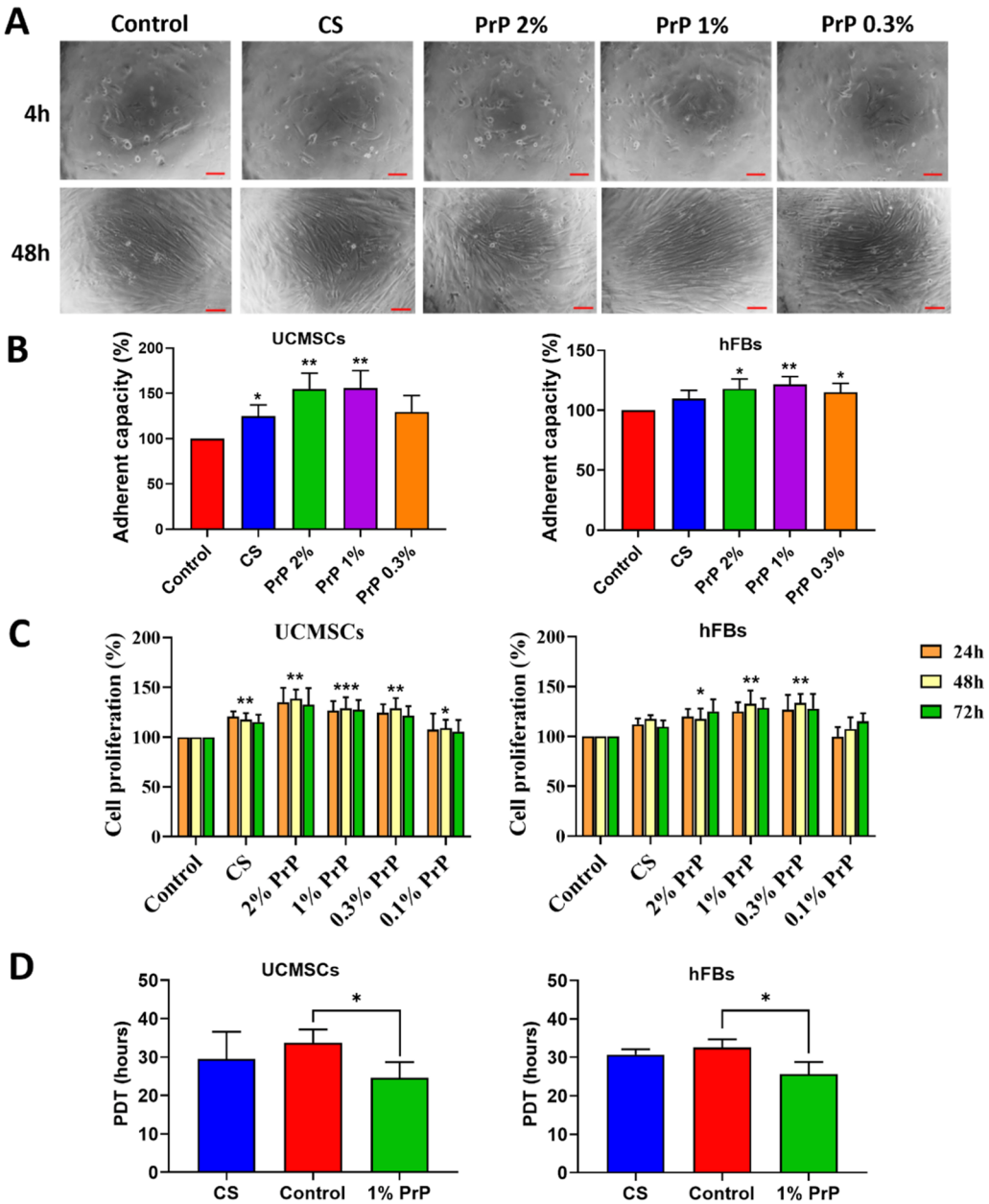

Fig. 2 UCB-PrP gels induced cellular adhesion and proliferation ($n = 3$). **A** Morphology of UCMSCs after seeding on 2D culture surface with 0.3 %, 1 %, and 2 % UCB-PrP gels at 4 h and 48 h in 2D cell cultures. **B** In 2D cell cultures, the adhesion capacity of UCMSCs and hFBs is induced by different concentrations of UCB-PrP gels. The 1 % and 2 % UCB-PrP gels reached the largest proportion of cells attached to the surface of culture dishes, and there was no difference between these two doses. **C** Cell proliferation of UCMSCs and hFBs using MTT assay induced by different concentrations of UCB-PrP gels as a coating substance. The concentration of 1 % UCB-PrP showed the best and most stable effects on both cell types. **D** Cell proliferation of UCMSCs and hFBs using the population doubling time (PDT) induced by 1 % UCB-PrP gels to coat the surface of cell culture flasks. Both cell types significantly doubled faster in the 1 % CB-PrP coated condition. CS: CELLStart™; *indicates $p < 0.05$; **indicates $p < 0.01$; ***indicates $p < 0.001$; ****indicates $p < 0.0001$

of dose–response growth curves was contrary between the two cell types, with the decrease in the UCB-PrP concentrations aligned with the increase of UCMSC growth (except the dose of 0.1 %) and the reduction of hFBs (Fig. 2C). These data indicated that UCB-PrP gels promoted the attachment and expansion of UCMSCs and hFBs. In both cell types, the 1% and 2 % CB-PrP gel concentrations displayed similar effects. Considering both efficacy and cost, we chose a dose of 1 % UCB-PrP gels for the subsequent evaluations.

Cell population doubling time (PDT) also indicates cell proliferation, where the lower the PDT, the higher the proliferation rate. The PDTs of UCMSCs (24.6 ± 4.1 h) and hFBs (25.6 ± 3.2 h) were significantly lower in the presence of 1% UCB-PrP gel coating substrate compared to the control of commercial CELLstart™ (29.5 ± 7.1 h and 30.7 ± 1.4 h, respectively) (Fig. 2D). These data imply that UCB-PrP gels could induce the growth of UCMSCs and hFBs. PDT results were consistent with the cell proliferation assessment using the MTT assay, as reported above.

UCB-PrP gels induced the alteration of the expression of some significant ECM-related genes

The cells' adherent capacity involves the production of extracellular matrix proteins. Thus, we next evaluated the mRNA expression of *COL1, COL3, HAS1, HA2, HAS3,* and *ELN* in UCMSCs and hFBs growing on different coating conditions. The results showed that the effects of UCB-PrP gels varied among these genes in two types of cells (Fig. 3).

Regarding UCMSCs, using UCB-PrP gels as a coating substrate significantly induced the expression of *HAS2* and Elastin genes compared to the controls and CELLstart™ in both 2D and 3D cultures. The higher expression of *ELN* was observed only in UCMSCs 2D (18.67 ± 0.72 fold change) and 3D (17.21 ± 1.65 fold change) cultures related to UCB-PrP gels, while *HAS2* was expressed higher in UCMSC monolayer associated with both UCB-PrP gels (6.75 ± 0.08 fold change) and CELLstart™ (5.81 ± 0.54 fold change) and UCMSC spheroids were 62.67 ± 23.5 fold change compared to those related to the controls, respectively ($p < 0.05$ and $p < 0.0001$). UCB-PrP gel did not induce the expression of *HAS3* in 3D culture. However, expression of *COL1* and *COL3* genes was also elevated in UCMSCs associated with CELLstart™ treatment ($p < 0.05$) compared to UCB-PrP gel treatment in both 2D and 3D cultures. However, *HAS1* was down-regulated in 2D cultures but up-regulated in 3D cultures in association with CELLstart™ treatment compared to UCB-PrP (2D: 0.53 ± 0.07 fold change vs 0.75 ± 0.1 fold change, 3D: 1.21 ± 0.08 fold change vs 0.73 ± 0.07 fold change, respectively) (Fig. 3 A, B).

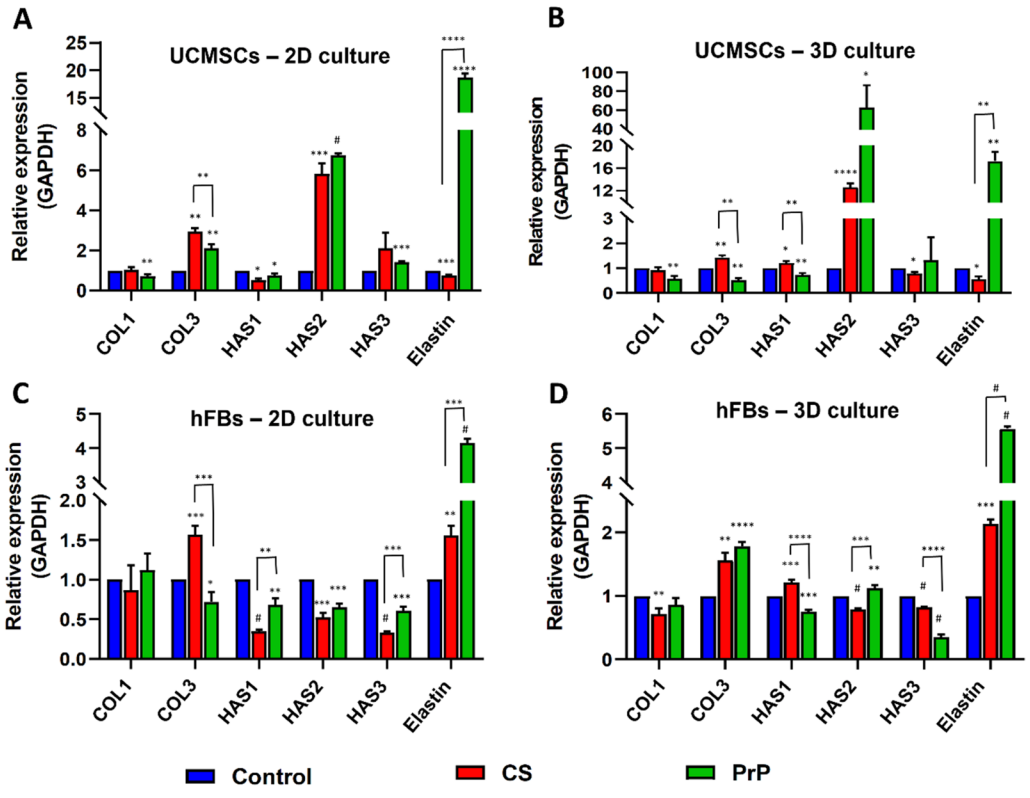

Fig. 3 Analysis of ECM-related gene expression in the UCB-PrP gel-treating conditions using qRT-PCR ($n = 3$). **A**, **B** Differential expression of ECM-related genes by UCMSCs in 2D and 3D cultures related to the surface coating culture flasks using UCB-PrP gels. **C**, **D** Differential expression of ECM-related genes by hFBs in 2D and 3D cultures related to the surface coating culture flasks using UCB-PrP gels. *indicates $p < 0.05$; **indicates $p < 0.01$; ***indicates $p < 0.001$; ****indicates $p < 0.0001$; #indicates $p < 0.00001$

Regarding hFB cultures, UCB-PrP gels only induced the higher expression of *ELN* (4.16 ± 0.11 fold change related to 2D cultures and 5.57 ± 0.07 fold change related to 3D) compared to the control and CELLstart™ in both 2D cultures (1.56 ± 0.12 fold change) and 3D cultures (2.13 ± 0.076 fold change) ($p < 0.001$) (Fig. 3C, D). Interestingly, in a 3D culture of hFBs, UCB-PrP gels promoted the expression of *COL3* (1.78 ± 0.07 fold change) and *HAS2* (1.12 ± 0.05 fold change) ($p < 0.01$) but reduced the expression of *HAS1* (0.75 ± 0.03 fold change), and *HAS3* (0.35 ± 0.04 fold change) in comparison with the control group ($p < 0.001$) (Fig. 3D). Meanwhile, compared to the control group, CELLstart™ induced the mRNA levels of *COL3* and *ELN* in both 2D (*COL3*: 1.57 ± 0.11 fold change, *ELN*: 1.56 ± 0.12 fold change) and 3D (*COL3*: 1.56 ± 0.12 fold change, *ELN*: 2.13 ± 0.076 fold change) culture conditions ($p < 0.01$) and HAS1 in 3D spheroids (1.21 ± 0.04 fold change) ($p < 0.001$) but inhibited the expression of *HSA2* and *HSA3* ($p < 0.001$) in both two culture conditions (Fig. 3C, D).

The data indicated that UCB-PrP gels could induce the expression of ECM-related genes, especially *ELN* and *HAS2*. The induction activities of UCB-PrP gels depended on the cell types and culture conditions.

UCB-PrP gels induced the multicellular spheroid fusion

The 3D culture represented the multi-interaction of cell-cell and cell-extracellular matrix (ECM). This model could perfectly reflect the capacity of UCB-PrP gels to promote cell adherence and ECM production. Data showed that the efficacy of spheroid formation in both UCMSCs (90 %) and hFBs (92 %) was significantly elevated associated with UCB-PrP gel-supplement cultures compared to the controls (UCMSC control: 62 %; hFB control: 70 %) (Fig. 4A). However, this efficacy was not different between UCB-PrP and commercial CELLstart™. In addition, the fusion of two spheroids when co-cultured in 3D conditions was also promoted using UCB-PrP gel (Fig. 4B, C). The quantitative evaluation of the fusion was based on the doublet length and doublet perimeter, as the less doublet length and perimeter indicated more fusion of spheroids. The data showed that in the UCB–PrP gel treatment, the doublets' length (UCMSCs: 66.28 ± 4.99 %, hFBs: 63.75 ± 5.71 %, at 72 h) (Fig. 4C) and perimeter (UCMSCs: 55.77 ± 3.63 %, hFBs: 55.52 ± 11.29 %, at 72 h) (Fig. 4D) were the lowest compared to that in CELLstart™ (doublets' length, UCMSCs: 73.78 ± 3.17 %, hFBs: 73.37 ± 7.0 %, at 72 h; perimeter, UCMSCs: 62.46 ± 5.19 %, hFBs: 81.79 ± 11.99 %, at 72 h) or the control (doublets' length, UCMSCs: 72.349 ± 3.21 %, hFBs: 75.59 ± 3.68.29 %, at 72 h; perimeter, UCMSCs: 64.17 ± 2.61 %, hFBs: 78.15 ± 4.66 %, at 72 h). These data indicate that supplementary UCB-PrP gels into the cell culture medium promoted the merging of the two adjacent spheroids.

UCB-PrP gels induced cell migration to close wounds in vitro

Based on cell adhesion and ECM gene expression results, we proposed the hypothesis that UCB-PrP gels may induce cell migration. Therefore, we performed the scratch assay in both hFBs and UCMSCs. The results showed that both UCMSCs and hFBs could migrate to close the scratch better related to using coating substance of UCB-PrP gels (UCMSCs: 98.5 ± 8.4 %, hFBs: 96.3 ± 6.4 %) and CELLstart™ (UCMSCs: 95.7 ± 12 %, hFBs: 92.7 ± 8.5 %) compared to the control (UCMSCs: 71.5 ± 7.2 %, hFBs: 62.8 ± 6.8 %) ($p < 0.05$ and $p < 0.01$) at 48 h. However, we observed that hFBs started migrating to close the wound faster from 24 h when they reached 66.7 ± 28.9 % associated with UCB-PrP gels (Fig. 5). These data indicate that the cell migration capacity of UCMSCs and hFBs was promoted by UCB-PrP gel that was treated as a coating substrate.

UCB-PrP gels induced skin wound healing in vivo

From the promising result of the in vitro scratching assay and spheroid combination, we investigated UCB-PrP gel's ability to support wound healing in the in vivo model. At 8 weeks, male rats were modeled with two similar wounded areas on their backs, one for UCB-PrP gel treatment and the other for betadine treatment as the control (Table 2). All rats were alive until the scheduled sacrifice for evaluation.

Daily observations showed that the UCB-PrP gel-treated wounds exhibited skin temperatures ranging from 37 °C to 37.5 °C, the skin color remained pink, the wound edges were dry and completely healed, and the incision surface was dry and covered in UCB-PrP gel-treated ones. In contrast, at wounded sites of the control group, the skin color turned dark, and wound edges were wet and not sealed at the end of the experiment. Moreover, ulcers were developed till day 14 in the control ones. The incision areas were quantitatively measured at days 3, 7, and 14 post-creation, and the results showed that the wounded area was significantly reduced in the UCB-PrP gel-treated groups compared to the controls. By day 14, the percentage of wound closure in UCB-PrP gel-treated wounds reached nearly 80 %, which was three times higher than the 27 % closure observed in controls (Fig. 6A).

Histological analysis indicated that, in both the UCB-PrP gels and controls, on day 3, the skin had a sizeable, ulcerated area with the surface a thick layer of necrotic pus tissue (yellow arrow), many neutrophils, and fibrin fibers (Fig. 6B). The ulcer base had a thin granulation

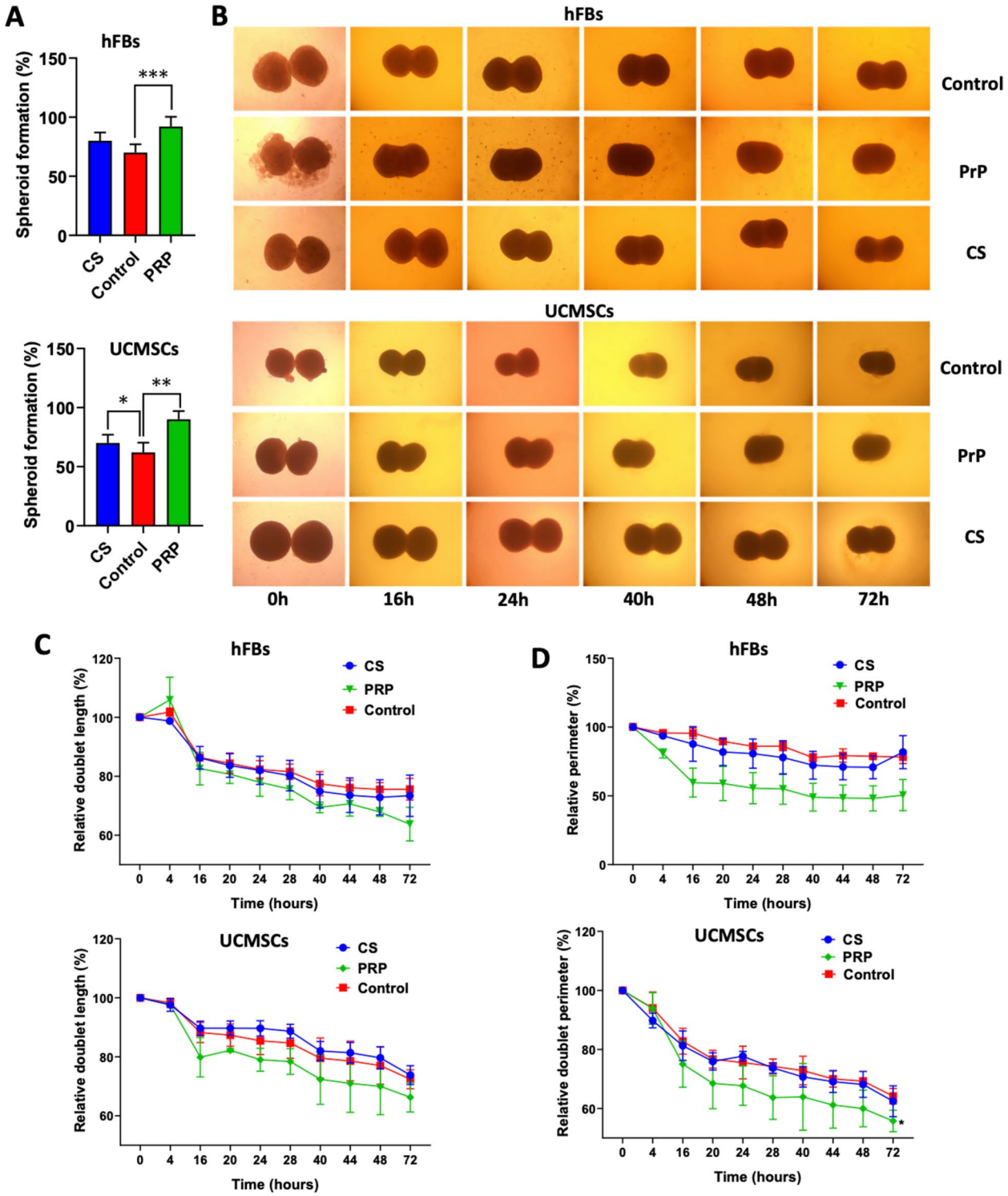

Fig. 4 Spheroid formation and fusion induction by UCB-PrP gels. **A** Spheroid formation efficacy of UCMSCs and hFBs, where the UCB-PrP gels owned the greatest capacity of spheroid formation and spheroid fusion ($n=5$). **B** Morphology of spheroid fusion at the time of UCB-PrP gel treatment ($n=5$). **C** Relative doublet length (%) by the time of UCB-PrP gel treatment ($n=3$). **D** Relative doublet perimeter (%) by the time of UCB-PrP gel treatment ($n=3$). *indicates $p<0.05$; **indicates $p<0.01$; ***indicates $p<0.001$

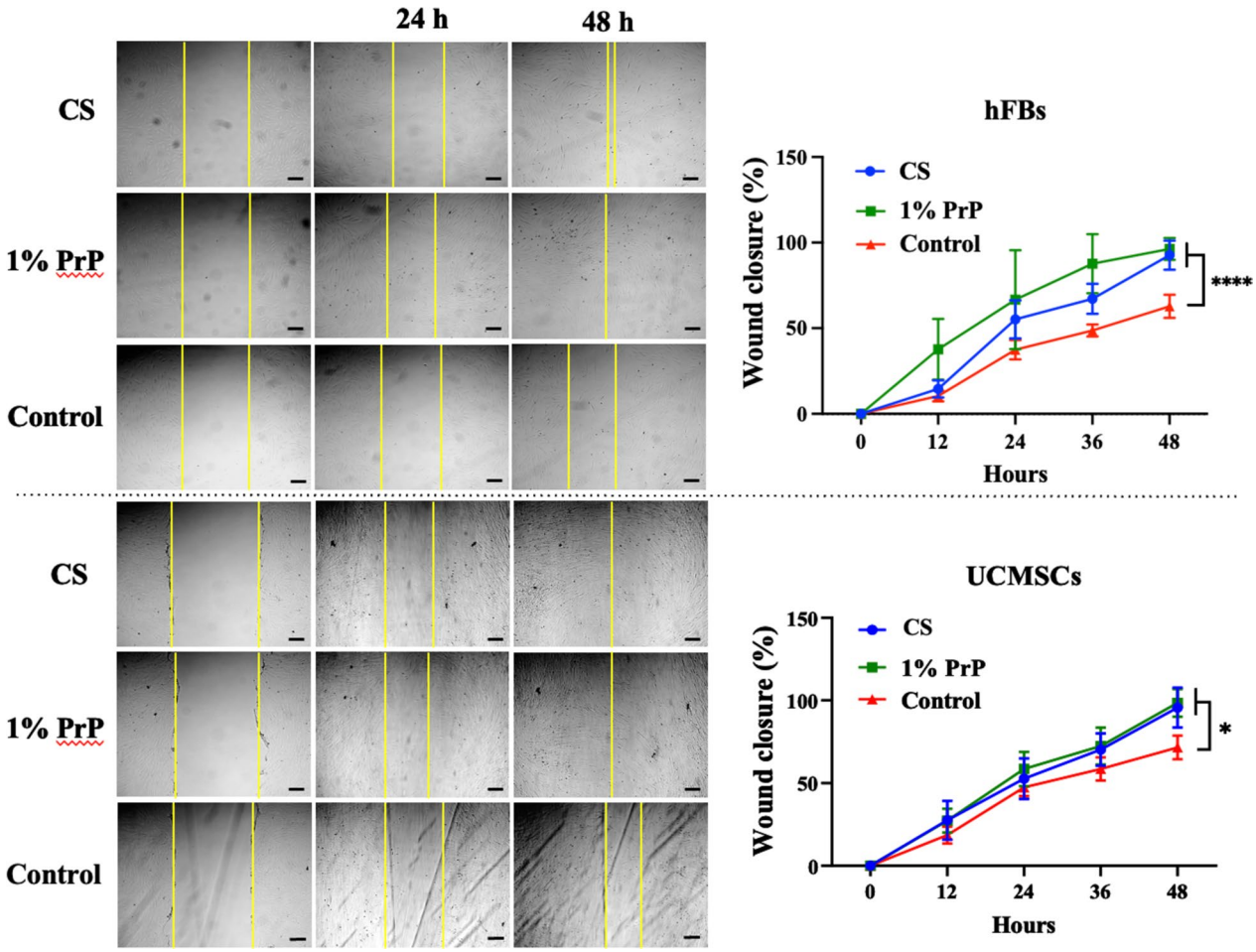

Fig. 5 Analysis of cell migration induced by UCB-PrP gels as a coating substrate using wound scratch assay ($n=3$). The images of hFBs and UCMSCs migrated to close the scratch wounds at different time points. Line charts showed the quantitative frequency of the wound cover (%) by hFBs or UCMSCs in relation to different time points. *indicates $p<0.05$; ****indicates $p<0.0001$

tissue with congested blood capillaries (black arrows), few fibroblasts, and many infiltrating neutrophils (red arrows). However, this status was maintained in the controls on day 7 and even day 14, accompanied by wound infection phenomenon in some cases. Interestingly, there was a significant change in the UCB-PrP gel treatment on day 7, with the narrowing of the ulcerated skin area. The ulcer surface had thin necrosis, and the bottom had a thick layer of granulation tissue, fibroblasts, and little infiltrating neutrophils. On day 14, the ulcerated area almost disappeared, with only a few infiltrated leukocytes (Fig. 6B). Taken together, the results demonstrated that UCB-PrP gel treatment significantly accelerated skin wound healing.

Table 2 General information on experimented rats

	Value (Mean ± SD)
Gender	Male
Age (weeks)	8.2 ± 0.2
Body weight (gram)	125.6 ± 6.1
Average wounded area (cm^2)	
The control sites	3.0 ± 0.1
UCB-PrP gel-treated sites	3.0 ± 0.2
Alive rate (%)	100

Discussion

The PrP gel is a well-known product that contains many growth factors and cytokines supporting cell development. Because of the ease of preparation, low immunogenicity, and high regenerative activities, PrP gels have been widely applied for treatment to support the healing of surgical operations and the treatment of degenerative diseases [1]. In addition, PrP facilitated cell attachment,

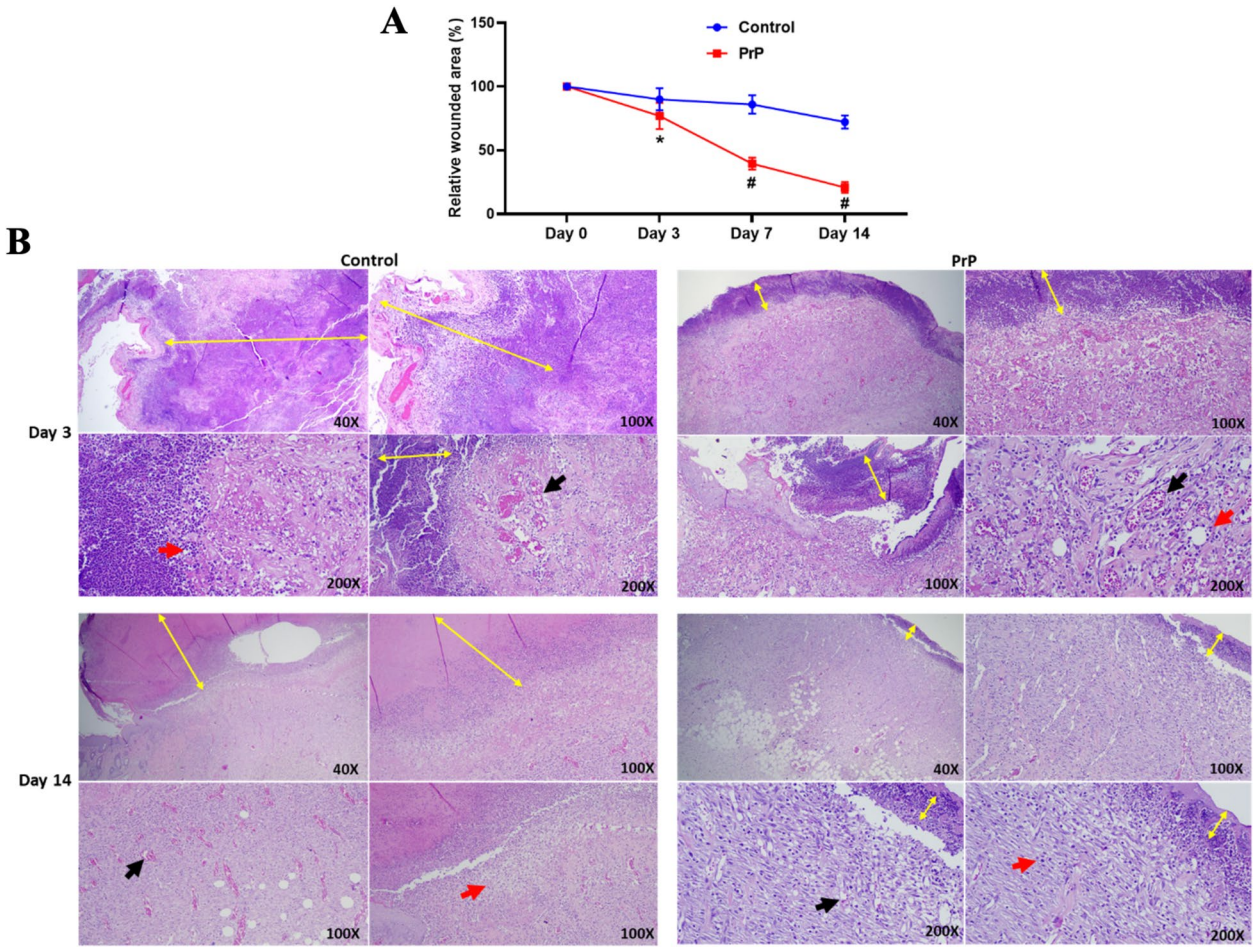

Fig. 6 UCB-PrP gels induced the wound healing in vivo ($n = 7$). **A** Area of wound sites (%) following the time of treatment. **B** Histological analysis of skin wound samples under UCB-PrP gel treatment and the controls. Necrotic pus tissue (yellow arrow); granulation tissue with congested blood capillaries (black arrows); Infiltrating neutrophils (red arrows). *indicates $p < 0.05$; #indicates $p < 0.00001$

proliferation, migration, and differentiation in 2D cultures has been reported [18, 19]. These achievements may be due to the PrP gels carrying bioactive factors that support the ability of cells to attach to the plastic surface. This means that PrP works as a coating substrate, allowing cell development. Thus, we examined UCB–PrP gels as a coating substrate for two adherent cell types, including hFBs and UCMSCs. Our data indicated that UCB-derived PrP gels enhanced cell adhesion, proliferation, and migration to close the scratched wounds in 2D cultures. This is similar to a previous report that using UCB-PrP gels as a supplement for cell cultures could enhance cell expansion and development [20]. In addition, cryopreserved UCB-PrP gels also induced the expression of bone morphogenetic protein-2 and osteoblastic differentiation by UCMSCs [21]. However, the use of PrP gels from peripheral blood and UCB as a substrate for plastic surface coating has yet to be investigated well, although many coating substrates based on ECM proteins have been commercialized for a particular or several cell types [22, 23].

As spheroids facilitate their functions, survivals, and efficacy regarding cell-based therapies or tissue engineering compared to single cells [24], forming spheroids is essential for the effectiveness of such types of therapy. Compared to single MSCs, MSC spheroids can survive better in harsh milieus and maintain their stemness [25], which differentiates into bone after being transfected into bone defects [26]. In addition, the chondrocyte spheroid is an appropriate biomaterial for 3D bioprinting to form 3D cartilage microtissues and may be used for vivo implantation [16]. Thus, if UCB-PrP gels can support spheroid formation, it will be an excellent solution for spheroid preparation for 3D printing or implantation because PRP gels are more biocompatible. Herein, we demonstrated that UCB-PrP gels enhanced spheroid formation and spheroid fusion by both hFBs and UCMSCs (Fig. 4). Thus, UCB-PrP gels, in general, and prepared by

the protocol described in this study, are potential candidates to improve spheroid formation. However, this product should be further examined for its functions in particular applications.

Interestingly, PrP gels could change gene expression, as previously mentioned [27, 28]. Using sequencing technique, Shen et al. reported that PrP gels upregulated cyclin-dependent kinase 1, polo-like kinase 1, cell division cycle 20, cyclin B1, aurora kinase B, and cyclin-dependent kinase 2, and downregulated v-myc avian myelocytomatosis viral oncogene homolog in human dermal papilla cells [27]. Autologous PrP gels could decrease *COL1* and *COL3* gene expression without affecting the *COL3/COL1* ratio and increase *MMP1* and *MMP3* expression by human tenocytes [28]. In the wounding context, PrP upregulated Notch pathway-related genes' expression, which plays a key role in the proliferation and differentiation of stem cells and angiogenesis in endothelial progenitor cells [29]. Different cells may respond differently to PrP, depending on the physiological conditions. In this study, we reported that UCB-PrP gels induced the expression of several ECM genes by hFBs and UCMSCs cultured in 2D and 3D conditions. The significance is that *ELN* mRNA was increased in all culture conditions and all cell types. However, other genes, such as *COL1*, *COL3*, *HAS1*, *HAS2*, and *HAS3,* responded to UCB-PrP treatment differently related to culture conditions and cell types. The current situation in which different cells respond variously to PrP observed in this study is superficial, and it requires more investigation on the factor triggering the expression of interested genes in the target cells, in addition to the downstream pathways in an association of cellular physiological properties and extracellular environments.

In addition to working as a substrate for plastic surface coating, UCB-derived PrP enriched with factors, including PDGF-BB, HGF, VEGF-A, and FGF-2 (Fig. 1B), that may be the additional reason for the better proliferation and migration of MSCs and hFBs. Previously, Tian et al. compared the growth factor expression levels in UCB-derived PrP and peripheral blood showed that a higher expression of VEGF-A and TIMP but lower expression of IGF, FGF-2, PDGF-AA/BB, and RANTES in UCB-derived PrP compared to the other PrP [30]. In addition, Lee et al. reported that the levels of PDGF-AB and TGF-β1 in UCB-derived PrP are higher than those in peripheral blood-derived PrP [20]. Thus, a comparison in the efficacy of PrP for osteoarthritis treatment has indicated that UCB-derived PrP gels improved the short term regarding VAS and HHS for 2 months [11]. The improvement score correlates to the disease severity, where the lower the osteoarthritis grade, the higher HHS improvement [11]. This may be due to the different levels of bioactive molecules in UCB-derived PrP gels, as described in the above study and this study. However, in this study, only several growth factors were investigated, and there was a lack of whole proteomic content. Investigating proteomics and metabolites in PRP is crucial for understanding its complex biological composition and identifying key proteins and bioactive molecules that drive its therapeutic effects. This knowledge enables scientists to standardize PRP formulations, optimize its efficacy for specific clinical applications, and uncover new mechanisms of action.

Previously, PrP has been investigated for the healing induction in vivo models. This biological product was safe and promoted wound healing through different mechanisms, for example, increasing re-epithelialization, angiogenesis, proliferation, and phagocytotic activities [7, 17, 31, 32]. In this study, UCB-derived PrP gels clearly promoted the wound healing process, both in vitro and in vivo models, and the repaired tissues were better completed (Figs. 5 and 6). UCB plasma derivatives have been investigated for regenerative applications, and then it suggested that UCB-derived plasma containing high levels of soluble factor of NKG2D ligands that reduced the production of INFγ by peripheral blood mononuclear cells and NKG2D and CD107a by immune cells [33]. Thus, UCB-derived PrP gels have been suggested for skin wound patches, while UCB-derived platelets and platelet poor plasma (PPP) have been proposed for severe ocular surface pathologies and inflammatory conditions, such as corneal ulcers or severe dry eye disease [33].

Few studies have compared autologous PrP and UCB-PrP for their efficacy in different diseases and their consistent and potential large-scale use. The main advantage of autologous PRP is its immunotolerant nature, but the quality varies depending on the patient's physiological conditions [34]. On the other hand, UCB-PrP is derived from women during reproductive age, which has reliable, safe, and more consistent therapeutic effects [35]. In this regard, the optimal impact of human PrP therapy is achievable when the plasma is obtained from younger women and blood sample processing is commercially standardized [36]. Indeed, compared to adult plasma, UCB plasma releases more growth factors and less pro-inflammatory cytokines [37–39]; in addition to a better improvement in human gingival and dermal fibroblast proliferation and migration in vitro, ovarian function in mice, endometrial damage in murine models, and osteoarthritis patients for the short term and patients with low osteoarthritic grade [11, 38, 40, 41]. Despite the reports on using PrP for clinical trials, there is a lack of direct comparison of the efficacy of UCB-PrP and autologous PrP, including this current study. In addition, there was a lack of an in-depth investigation of the mechanisms

herein. Thus, it requires a more comprehensive and contextualization of the effect of PrP on the biological activity of cells and in vivo models related to PrP sources. In addition, to advance the UCB-derived PrP product prepared in this study toward practical application, it should be evaluated in human tissues and clinical trials.

Conclusion

Data from this study showed that UCB-derived PrP gels enriched with growth factors and then facilitated cell attachment and spheroid formation. That UCB-derived PrP gels increased the spheroid formation and fusion by both UCMSCs and hFBs reveals the novel application of these PrP gels as a substrate to prepare effectively biomaterial spheroids for 3D printing or engraftment. In addition, UCB-derived PrP gels promote UCMSC and hFB proliferation and migration in vitro and wound healing in animal models. These data indicate that UCB-derived PrP gels may be a potential alternative to autologous peripheral blood-derived PrP gels for wound healing treatment. Despite the limitation of this study is the un-fully characterization of UCB-derived PrP gels regarding their bioactive components and mechanism under their functions, the data confirm the role of PrP in wound healing in addition to the novel application of UCB-derived PrP as a substrate for cell attachment for other medication applications.

Abbreviations

COL	Collagen
ELN	Elastin
FGF-2	Fibroblast growth factor
HAS	Hyaluronan synthase
hFB	Human fibroblasts
HGF	Hepatocyte growth factor
HHS	Harris hip score
IGF	Insulin-loke growth factor
NKG2D	Natural killer group 2D
MSCs	Mesenchymal stem cells
PDGF–BB	Platelet-derived growth factor–BB
PrP	Platelet riched plasma
RANTES	Regulated upon activation, normal T cell expressed and presumably secreted
TGF-β1	Transforming growth factor beta 1
UCB	Umbilical cord blood
UCMSC	Umbilical cord-derived mesenchymal stem cells
VAS	Visual analogue scale
VEGF-A	Vascular endothelial growth factor A

Author contributions

T-H.T., U.T.T.T., N.T.M.H., X-H.N., N.H.N.: the conception and design of the study; T-H.T., U.T.T.T., T-T.N., B-H.P., Q-D.L., N.T.M.H., T-H.N., X-H.D.: data collection; T-H.T., U.T.T.T., N.H.N., T-T.N., B-H.P., Q-D.L., N.T.M.H., T-H.N., X-H.N., X-H.D.: analysis and interpretation of data; T-H.T., U.T.T.T., T-H.N., Q-D.L., N.T.M.H.: manuscript drafting; N.T.M.H., X-H.N., N.H.N.: manuscript revising; U.T.T.T.: final approval.

Funding

This project was funded by the Vingroup Innovative Foundation (VinIF), project number: VINIF.2021.DA00193. This source has no involvement in the study design, collection, analysis, and interpretation of data, in the writing of the manuscript, and in the decision to submit the manuscript for publication.

Data availability

No datasets were generated or analysed during the current study.

Declarations

Ethics approval and consent to participate

Umbilical cord blood samples were collected following the protocols approved by the Vinmec International General Hospital Joint Stock Company's ethics committee (Ethical approval number: 02/2022/CN-HĐĐĐ VMEC) in compliance with the Helsinki Declaration. All donors signed written informed consent before donating their samples. The use of animals and all experimental protocols involving animals in this study followed guidelines for animal treatment and complied with the relevant legislation from the Institutional Review Board at Dinh Tien Hoang Institute of Medicine (Ethical approval number: IRB-A 2203).

Competing interests

The authors declare no competing interests.

Author details

[1]National Burn Hospital, Hanoi 100000, Vietnam. [2]Department of Practical and Experimental Surgery, Vietnam Military Medical University, 160 Phung Hung Street, Phuc La, Ha Dong, Hanoi, Vietnam. [3]VNU University of Science, Vietnam National University, Hanoi 100000, Vietnam. [4]Vinmec Hi-Tech Center, Vinmec Healthcare System, 458 Minh Khai, Hai Ba Trung, Hanoi 100000, Vietnam. [5]Vinmec-VinUni Institute of Immunology, College of Health Sciences, VinUniversity, Hanoi 100000, Vietnam. [6]College of Health Sciences, VinUniversity, Hanoi 100000, Vietnam.

Received: 29 August 2024 Accepted: 14 February 2025
Published: 28 February 2025

References

1. Collins T, Alexander D, Barkatali B. Platelet-rich plasma: a narrative review. EFORT Open Rev. 2021;6(4):225–35.
2. Abdullah BJ, Atasoy N, Omer AK. Evaluate the effects of platelet rich plasma (PRP) and zinc oxide ointment on skin wound healing. Ann Med Surg. 2012;2019(37):30–7.
3. Tang YQ, Yeaman MR, Selsted ME. Antimicrobial peptides from human platelets. Infect Immun. 2002;70(12):6524–33.
4. Bielecki T, Gaździk TS, Arendt J, Szczepański T, Krol WL, Wielkoszyński T. Antibacterial effect of autologous platelet gel enriched with growth factors and other active substances: an in vitro study. J Bone Joint Surg Br Vol. 2007;89(3):417–20.
5. Kolimi P, Narala S, Nyavanandi D, Youssef AAA, Dudhipala N. Innovative treatment strategies to accelerate wound healing: trajectory and recent advancements. Cells. 2022;11(15):2439.
6. Verma R, Kumar S, Garg P, Verma YK. Platelet-rich plasma: a comparative and economical therapy for wound healing and tissue regeneration. Cell Tissue Bank. 2023;24(2):285–306.
7. Griffeth RJ, García-Párraga D, Mellado-López M, Crespo-Picazo JL, Soriano-Navarro M, Martinez-Romero A, Moreno-Manzano V. Platelet-rich plasma and adipose-derived mesenchymal stem cells for regenerative medicine-associated treatments in bottlenose dolphins (*Tursiops truncatus*). PLoS ONE. 2014;9(9): e108439.
8. Buzzi M, Versura P, Grigolo B, Cavallo C, Terzi A, Pellegrini M, Giannaccare G, Randi V, Campos E. Comparison of growth factor and interleukin content of adult peripheral blood and cord blood serum eye drops for cornea and ocular surface diseases. Transfus Apheres Sci. 2018;57(4):549–55.
9. Murphy MB, Blashki D, Buchanan RM, Yazdi IK, Ferrari M, Simmons PJ, Tasciotti E. Adult and umbilical cord blood-derived platelet-rich plasma for mesenchymal stem cell proliferation, chemotaxis, and cryo-preservation. Biomaterials. 2012;33(21):5308–16.
10. Masuki H, Okudera T, Watanebe T, Suzuki M, Nishiyama K, Okudera H, Nakata K, Uematsu K, Su CY, Kawase T. Growth factor and pro-inflammatory cytokine contents in platelet-rich plasma (PRP), plasma rich in

growth factors (PRGF), advanced platelet-rich fibrin (A-PRF), and concentrated growth factors (CGF). Int J Implant Dent. 2016;2(1):19.
11. Mazzotta A, Pennello E, Stagni C, Del Piccolo N, Boffa A, Cenacchi A, Buzzi M, Filardo G, Dallari D. Umbilical cord PRP vs. autologous PRP for the treatment of hip osteoarthritis. J Clin Med. 2022;11(15):4505.
12. Kisiel MA, Klar AS. Isolation and culture of human dermal fibroblasts. Methods Mol Biol. 2019;1993:71–8.
13. Hoang DH, Nguyen TD, Nguyen HP, Nguyen XH, Do PTX, Dang VD, Dam PTM, Bui HTH, Trinh MQ, Vu DM, Hoang NTM, Thanh LN, Than UTT. Differential wound healing capacity of mesenchymal stem cell-derived exosomes originated from bone marrow, adipose tissue and umbilical cord under serum- and xeno-free condition. Front Mol Biosci. 2020;7:119.
14. Le HM, Nguyen LT, Hoang DH, Bach TQ, Nguyen HTN, Mai HT, Trinh DP, Nguyen TD, Nguyen LT, Than UTT. Differential development of umbilical cord-derived mesenchymal stem cells during long-term maintenance in fetal bovine serum-supplemented medium and xeno- and serum-free culture medium. Cell Reprogram. 2021;23(6):359–69.
15 Ghasemi M, Turnbull T, Sebastian S, Kempson I. The MTT assay: utility, limitations, pitfalls, and interpretation in bulk and single-cell analysis. Int J Mol Sci. 2021;22(23):12827.
16. De Moor L, Fernandez S, Vercruysse C, Tytgat L, Asadian M, De Geyter N, Van Vlierberghe S, Dubruel P, Declercq H. Hybrid bioprinting of chondrogenically induced human mesenchymal stem cell spheroids. Front Bioeng Biotechnol. 2020;8:484.
17. Xu P, Wu Y, Zhou L, Yang Z, Zhang X, Hu X, Yang J, Wang M, Wang B, Luo G, He W, Cheng B. Platelet-rich plasma accelerates skin wound healing by promoting re-epithelialization. Burns Trauma. 2020;8: tkaa028.
18. Wu Y-D, Jiang H-J, Zhou H-H, Xu J-Y, Liu Q, Sun X-H, Wu Y-H, Lin Z-Y. PRP significantly promotes the adhesion and migration of vascular smooth muscle cells on stent material. Eur J Med Res. 2023;28(1):581.
19. Carter CA, Jolly DG, Worden CE, Hendren DG, Kane CJM. Platelet-rich plasma gel promotes differentiation and regeneration during equine wound healing. Exp Mol Pathol. 2003;74(3):244–55.
20. Lee J-Y, Nam H, Park Y-J, Lee S-J, Chung C-P, Han S-B, Lee G. The effects of platelet-rich plasma derived from human umbilical cord blood on the osteogenic differentiation of human dental stem cells. In Vitro Cell Dev Biol Anim. 2011;47:157–64.
21. Baba K, Yamazaki Y, Sone Y, Sugimoto Y, Moriyama K, Sugimoto T, Kumazawa K, Shimakura Y, Takeda A. An in vitro long-term study of cryopreserved umbilical cord blood-derived platelet-rich plasma containing growth factors—PDGF-BB, TGF-β, and VEGF. J Cranio-Maxillofac Surg. 2019;47(4):668–75.
22. InCelligence. Coating (surface treatment) of cell culture plastic 2024. https://incelligence.de/en/cell-culture/cell-culture-plastic-ware/coating-surface-treatment. Accessed 4 Jan 2024.
23. Cooke MJ, Phillips SR, Shah DSH, Athey D, Lakey JH, Przyborski SA. Enhanced cell attachment using a novel cell culture surface presenting functional domains from extracellular matrix proteins. Cytotechnology. 2008;56(2):71–9.
24. Lee NH, Bayaraa O, Zechu Z, Kim HS. Biomaterials-assisted spheroid engineering for regenerative therapy. BMB Rep. 2021;54(7):356–67.
25. Murphy KC, Fang SY, Leach JK. Human mesenchymal stem cell spheroids in fibrin hydrogels exhibit improved cell survival and potential for bone healing. Cell Tissue Res. 2014;357(1):91–9.
26. Ho SS, Keown AT, Addison B, Leach JK. Cell migration and bone formation from mesenchymal stem cell spheroids in alginate hydrogels are regulated by adhesive ligand density. Biomacromol. 2017;18(12):4331–40.
27. Shen H, Cheng H, Chen H, Zhang J. Identification of key genes induced by platelet-rich plasma in human dermal papilla cells using bioinformatics methods. Mol Med Rep. 2017;15(1):81–8.
28. de Mos M, van der Windt AE, Jahr H, van Schie HTM, Weinans H, Verhaar JAN, van Osch GJVM. Can platelet-rich plasma enhance tendon repair?: a cell culture study. Am J Sports Med. 2008;36(6):1171–8.
29. Zhang C, Zhu Y, Lu S, Zhong W, Wang Y, Chai Y. Platelet-rich plasma with endothelial progenitor cells accelerates diabetic wound healing in rats by upregulating the Notch1 signaling pathway. J Diabetes Res. 2019;2019:5920676.
30. Tian J, Li XJ, Ma Y, Mai Z, Yang Y, Luo M, Xu W, Chen K, Chen X, Tang J, Cheng B, Cui X. Correlation of bioactive components of platelet rich plasma derived from human female adult peripheral blood and umbilical cord blood with age. Sci Rep. 2023;13(1):18428.
31. Myung H, Jang H, Myung JK, Lee C, Lee J, Kang J, Jang W-S, Lee S-J, Kim H, Kim H-Y, Park S, Shim S. Platelet-rich plasma improves the therapeutic efficacy of mesenchymal stem cells by enhancing their secretion of angiogenic factors in a combined radiation and wound injury model. Exp Dermatol. 2020;29(2):158–67.
32. Suthar M, Gupta S, Bukhari S, Ponemone V. Treatment of chronic non-healing ulcers using autologous platelet rich plasma: a case series. J Biomed Sci. 2017;24(1):16.
33. Samarkanova D, Cox S, Hernandez D, Rodriguez L, Casaroli-Marano RP, Madrigal A, Querol S. Cord blood platelet rich plasma derivatives for clinical applications in non-transfusion medicine. Front Immunol. 2020;11:942.
34. Le ADK, Enweze L, DeBaun MR, Dragoo JL. Platelet-rich plasma. Clin Sports Med. 2019;38(1):17–44.
35. Caiaffa V, Ippolito F, Abate A, Nappi V, Santodirocco M, Visceglie D. Allogenic platelet concentrates from umbilical cord blood for knee osteoarthritis: preliminary results. Med Glas. 2021;18(1):260–6.
36. Castellano JM, Mosher KI, Abbey RJ, McBride AA, James ML, Berdnik D, Shen JC, Zou B, Xie XS, Tingle M, Hinkson IV, Angst MS, Wyss-Coray T. Human umbilical cord plasma proteins revitalize hippocampal function in aged mice. Nature. 2017;544(7651):488–92.
37. Parazzi V, Lazzari L, Rebulla P. Platelet gel from cord blood: a novel tool for tissue engineering. Platelets. 2010;21(7):549–54.
38. Mani R, Roopmani P, Rajendran J, Maharana S, Giri J. Cord blood platelet rich plasma (PRP) as a potential alternative to autologous PRP for allogenic preparation and regenerative applications. Int J Biol Macromol. 2024;262:129850.
39. Ehrhart J, Sanberg PR, Garbuzova-Davis S. Plasma derived from human umbilical cord blood: potential cell-additive or cell-substitute therapeutic for neurodegenerative diseases. J Cell Mol Med. 2018;22(12):6157–66.
40 Buigues A, Marchante M, de Miguel-Gómez L, Martinez J, Cervelló I, Pellicer A, Herraiz S. Stem cell-secreted factor therapy regenerates the ovarian niche and rescues follicles. Am J Obstet Gynecol. 2021;225(1):65.e1-e14.
41. de Miguel-Gómez L, López-Martínez S, Campo H, Francés-Herrero E, Faus A, Díaz A, Pellicer A, Domínguez F, Cervelló I. Comparison of different sources of platelet-rich plasma as treatment option for infertility-causing endometrial pathologies. Fertil Steril. 2021;115(2):490–500.

Publisher's Note